TURBULENT FLOW, HEAT AND MASS EXCHANGE IN INDUSTRIAL INDUCTION CHANNEL FURNACES WITH VARIOUS CHANNEL DESIGN, IRON YOKE POSITION AND CLOGGING

S. Pavlovs[(1)], A. Jakovics[(1)], D. Bosnyaks[(1)], E. Baake[(2)], B. Nacke[(2)]

[(1)]Laboratory for Mathematical Modelling of Environmental and Technological Processes, University of Latvia, 8 Zellu str., LV-1002, Riga

[(2)]Institute of Electrotechnology, Leibniz University of Hannover Wilhelm-Busch-Str. 4, D-30167 Hannover, Germany

The *induction channel furnace* (ICF) is industrial metallurgical equipment with high electrical and thermal efficiency and is used for melting, holding and casting of metals and alloys.

Damages like erosion, clogging and infiltration of the ceramic lining in the channel as well as local overheating in the channel may lower the cleanness of the processed melt as well as the effectiveness and safety of ICF operation.

The way to minimize these known problems is the choice of efficient regimes of melt circulation in ICF channel to provide controlled intensification of turbulent heat exchange between channel and throat.

1. Temperature maximum and its position in ICF channel

The current paper presents the further development of long-term computations [1–5] for industrial ICF. The target is large time scale processes in the flow.

The considered ICF models have identical electrical induced power in the melt ($\approx 215kW$) and geometry, which differs from the original design [4] with two symmetric branches of the channel (Figure 1a) as follows:

√ *Model (i) with widened channel branch* (Figure 1b) has gradual expansion of left channel branch from 100% to 200% of cross-sectional area at the junction to the throat [4].

√ *Model (ii) with moved iron yoke* (Figure 1c) is a modification of the model (i) with widened channel branch. It is introduced by a clockwise rotation by 90º angle of iron yoke from the original position, which is located around the right branch of channel at an angle $\alpha = -45^{\circ}$, to the new one $\alpha = 45^{\circ}$.

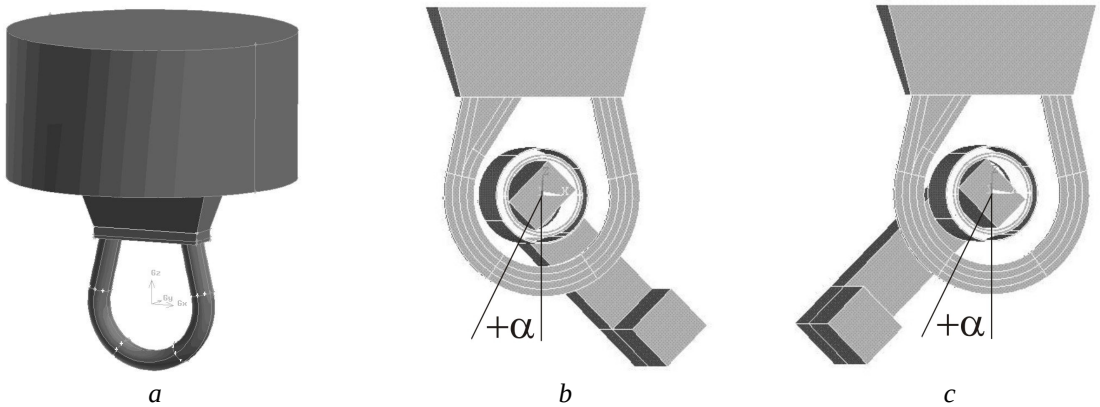

a *b* *c*

Figure 1. Original design of ICF with symmetrical channel (a). Geometry of ICF with left widened branch of channel for EM modelling: (b) original position ($\alpha = -45^{\circ}$) of iron yoke; (c) moved iron yoke ($\alpha = 45^{\circ}$).

To retrace, the top part of ICF is a large cylindrical melt vessel or bath (Figure 1a), which is taken into account only in hydrodynamic (HD) and thermal modelling. The bottom part of ICF consists of channel, throat, inductor and iron yoke (Figures 1b, 1c), which are taken into account in electromagnetic (EM) modelling. The origin of Cartesian coordinate system is placed at the geometrical centre of the ICF channel loop, where x-axis corresponds to the long side of the channel, y-axis – to the short, z-axis – to the vertical direction. The central angle α is counting clockwise as shown in the Figures 1b, 1c starting with an intersection of two perpendicular cross-sections y = 0 and x = 0.

The numerical simulations are performed using commercial software packages *ANSYS* for EM field and *FLUENT* for HD and temperature field. The initial distributions of the melt velocity and temperature are obtained using steady state 3D standard *k-ε* model. For further computations the transient 3D *Large Eddy Simulation* (LES) model of turbulence is used. The mesh for HD computations consists of approximately 6 million elements. The time step for transient HD computations is chosen as 0.005 sec. Computation time to obtain 1 sec of physical flow at PC cluster with 16 processor cores is 36–54 hours. For post-processing of profile files prepared by FLUENT an own developed code is used [2].

The validity of *LES* approach has been verified by means of experimental and computational results' comparison obtained using experimental setups and ICF models. Then verified *LES* approach has been applied for long-term computations of industrial ICF properties [1–5].

The peculiarities of model (ii). The long-term oscillations of temperature maximum in the channel T_{max} and its position α for original model with symmetrical branches (Figure 1a) and model (i) with widened left channel branch (Figure 1b) are considered in details in [2,5].

The main idea of model (ii) with moved position of iron yoke (Figure 1c) is a combination of two factors which influence the value and position of temperature maximum in ICF channel:

√ the widening of the left channel branch (Figure 1b) of ICF ensures the better conditions for thermal-gravitational convection (TGC) development in comparison with the ICF design with symmetrical channel branches (Figure 1a) and, consequently, the possibility for more intensive heat exchange in this branch of channel;

√ the position of moved iron yoke of inductor (Figure 1c) ensures that maxima of EM force and Joule heat density (see Figure 5 in [5]) are obtained in the widened branch of channel with better conditions for TGC development.

Therefore both non-symmetrical factors are combined now in one channel branch.

The choice of initial conditions for the model (ii). The distributions of HD and thermal fields for ICF with widened channel branch and original yoke position for the flow time t = 63 sec (Figure 2a) have been chosen as the initial conditions. The reasons for the choice are the following – the flow time point t = 63 sec corresponds to the local maximal value of T_{max} and belongs to the range of flow time, which is the quasi-stable for position of T_{max} in the channel.

Comparison of results for models (ii) and (i) are shown in Figure 2, which are plotted using 23 000 points, i.e. every 0.005 sec of the flow time in the range 60–175 sec.

The estimated time, when a model (ii) has "forgotten" about its initial conditions used from the basic model (i), is t ~ 75 sec.

The value T_{max} of temperature maximum for the model (ii). The value of T_{max} is oscillating around time-averaged temperature T_{max}^{aver} ~1803.1 K with deviations ±5.35 K for flow time t = 65–175 sec with main period of oscillations $t_{oscil}^{T_{max}}$ ~ 55 sec.

The obtained T_{max} extremes are the following – the maximum ~1807.7 K at t ≈ 116 sec and the minimum ~1797 K at t ≈ 139 sec (Figure 2b).

The position α of temperature maximum for the model (ii). The T_{max} position is mainly in the channel branch with largest cross-section area – the maximum value of the angle is $\alpha_{max} \sim 134^o$.

The permanent presence of T_{max} position for the flow times period t ~ 105–115 sec as well as short presence for flow time periods t ~ 93–105 and 145–160 sec is obtained in the right branch of channel with the range of α from 0º till −55º (Figure 2b).

The averaged value of angle is $\alpha_{aver} \sim 44.5^o$.

The periods of the low-frequency oscillations of position α of T_{max} is $t^{\alpha}_{oscil} \sim 55$ sec, that is the same with $t^{T_{max}}_{oscil}$.

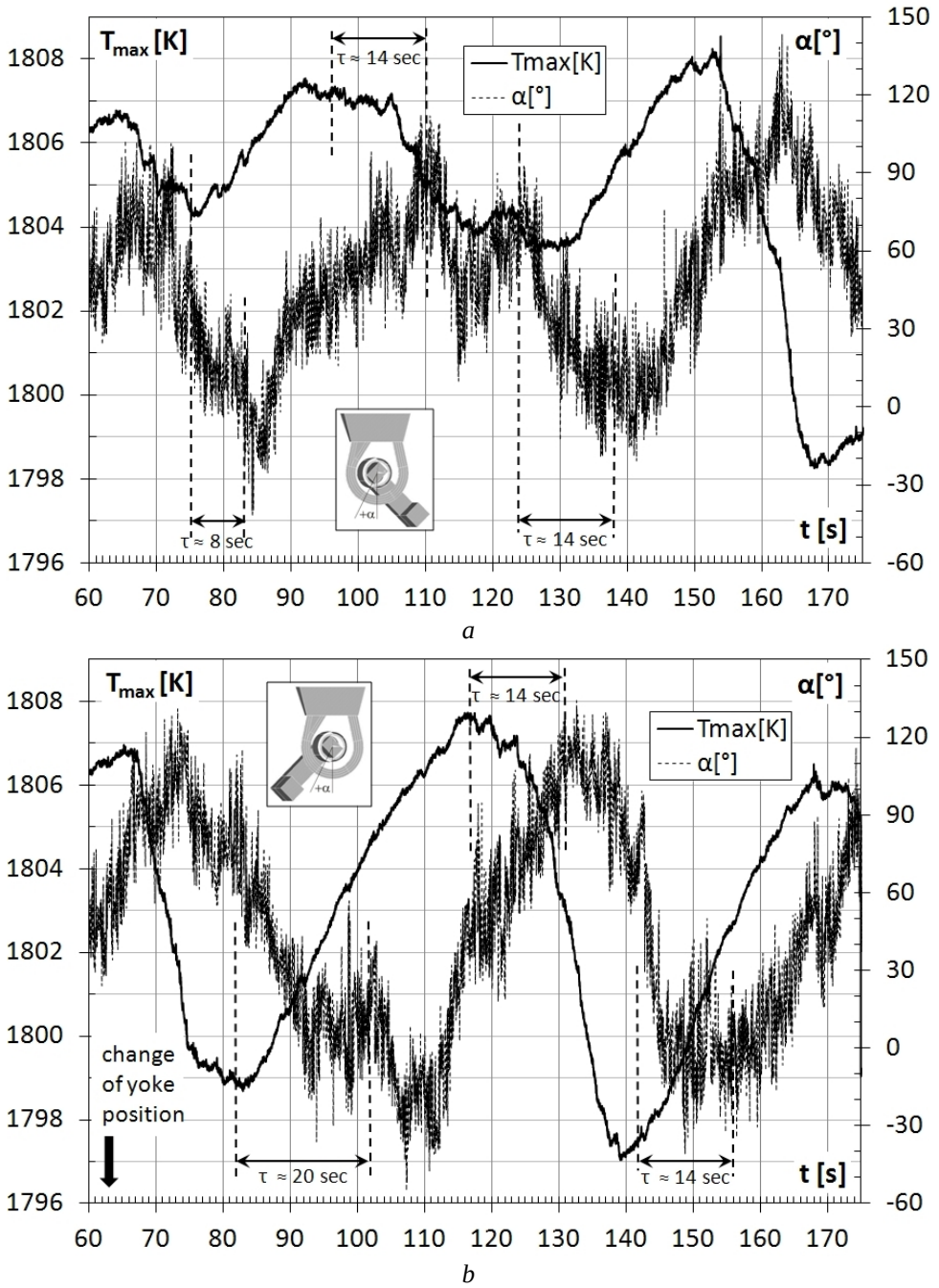

Figure 2. Maximal temperature T_{max} and angle α of its position in ICF with widened channel (y = 0) for flow time t = 60–175 sec: (a) original yoke α = –45º; (b) moved yoke α = 45º.

Time delay between extremes of T_{max} position α and T_{max} itself for the model (ii). The analysis of both curves in Figure 2b shows the time delay of α extremes (both maxima and minima) relative to according T_{max} extremes. The time delay value is τ ~ 14 sec for the flow time after 100 sec as well as τ ~ 20 sec for interval of flow time from 60 sec till 100 sec.

The explanation of this phenomenon is concerned with inertia of melt reaction to increasing of buoyancy force at higher temperature differences or decreasing of buoyancy force at lower temperature differences – displacement of more heated melt closer to outlet of channel's left branch or displacement of less heated melt closer to channel loop's lower region.

Differences in results for model (ii) and model (i). The comparison of results for ICF with moved iron yoke (Figure 2b) and for ICF with a widened channel branch (Figure 2a) show the following:

√ The main periods of oscillations of T_{max} and α are equal ~ 55 sec for both models;

√ Time delays between extremes of T_{max} position α and T_{max} itself are equal ~ 14 sec for both models for the flow time interval after 90–100 sec, but for flow time interval from 60 sec till 90–100 sec time delay for model (ii) is 2 times greater than for model (i) – compare 20 sec and 8 sec (Figure 2).

√ Time-averaged temperature T_{max}^{aver} ~1802.7 K for model (ii) is slightly less than time-averaged temperature T_{max}^{aver} ~1804.9 K for model (i).

Deviations of temperature during oscillations for time flow interval from 60 sec till 160 sec are greater for model (ii) than for model (i) – compare ±5.35 K and ±2.6 K. If time flow interval from 160 sec till 175 sec is taken into account, the deviations of temperature for model (i) increase till ±5.15 K and became similar to model (ii).

Conclusions:

– ICF construction with moved yoke provides the smaller overheating temperature in the channel in comparison with the basic model with the original yoke position.

– The combination of both non-symmetrical factors (channel branch widening as well as iron yoke position changing) in one channel branch results the long-term pulsations with more regular amplitude for all considered flow time interval.

2. Influence of ICF clogging on velocity and temperature field

During the long-term operation of ICF the formation of non-conductive sediments on different ICF construction elements occurs. These sediments noticeably change the furnace geometry. This is the cause of prolongation of induced current loops in the melt as well as is the cause of changes of hydraulic resistance.

In order to illustrate the influence of non-conductive sediments on velocity and temperature field several models of ICF with sediments on the bottom of throat are chosen.

The considered ICF models have identical current in inductor (1850 A) and are built on the base of *original model* of ICF with symmetrical channel and iron yoke position at α = 45º (Figure 3a):

√ *IFC with sediments at bottom of throat in form of "hill"* (Figure 3b) – *model (1)*;

√ *IFC with sediments at bottom of throat in form of "bank"* (Figure 3c) – *model (2)*.

The introduction of Cartesian coordinate system is described above.

The numerical simulations are performed using commercial software packages *ANSYS* for EM field and *CFX* for HD and temperature field. Melt velocity and temperature are obtained using 3D Shear Stress Transport (SST) k-ω model of turbulence. The y=0 plane is considered as symmetry plane, thus EM and HD computations are performed for the half of ICF geometry. The mesh for ED computations consists of 300–350 hundred elements, the

mesh for HD computations – 1–1.5 million elements. Computations have been performed using 4–6 processor cores of desktop PC or 8 cores of PC cluster.

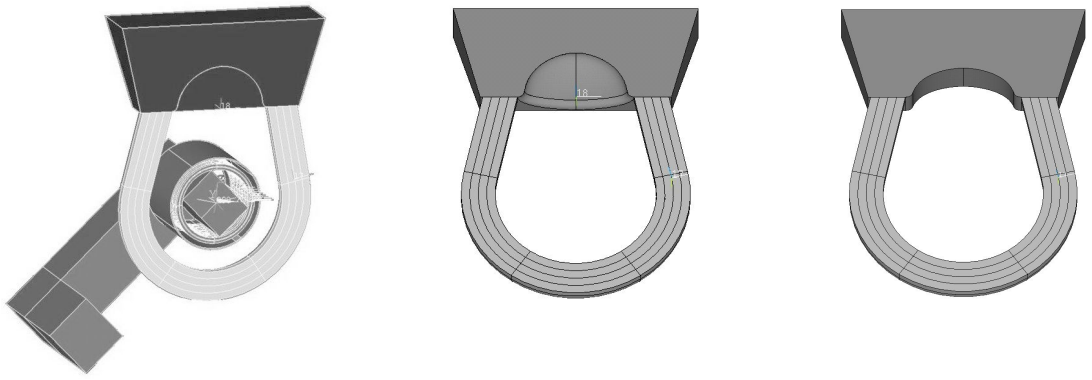

a *b* *c*

Figure 3. Original model of ICF with symmetrical channel and iron yoke position at α = 45º (a). Model 1 with sediments in form of "hill" (b). Model 2 with sediments in form of "bank" (c).

Joule heat. The distribution of the Joule heat in the channel loop is similar for all three models (Figure 4a, 4b, 4c). The values of Joule heat density at bottom of inner surface of channel loop are very closed (Table 1).

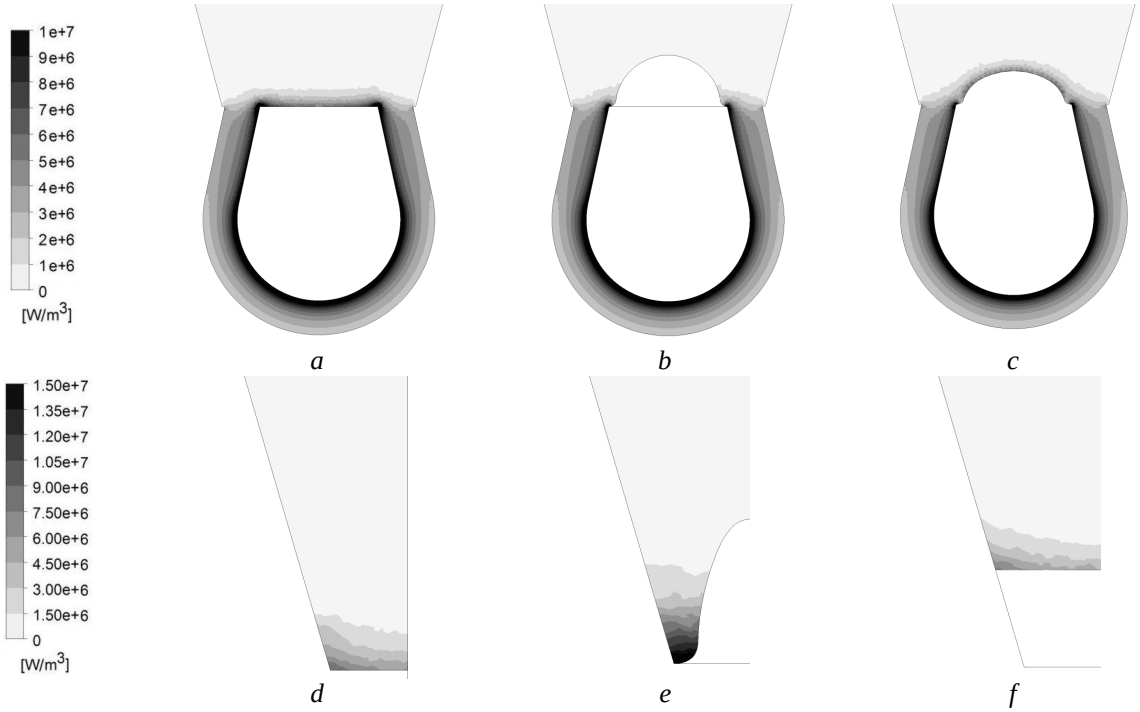

a *b* *c*

d *e* *f*

Figure 4. Joule heat power density distribution for original model (a,d), model 1 (b,e) and model 2 (c,f) for cross-sections y=0 (a,b,c) as well as for cross-section x=0 (d,e,f) in zone of throat with sediments.

The distributions in side cross-section x=0 show the concentration of Joule heat at the bottom of the interface of sediments and slant surface of throat of model 1 (Figure 4e). Maximal value of Joule heat density $1.9 \cdot 10^7$ W/m^3 is ≈ 13% greater in comparison with original model (Table 1).

The greatest integral value of Joule heat power in the melt 236.6 kW (Table 1) is for model 1 – it is for ≈2% greater than for original model. The smallest one is for model 2 – it is ≈ 1.7% smaller than for original model.

Table 1. Characteristic parameter of models

Model	Integral Joule heat power [kW]	Joule heat power density [10^7·W/m^3]		Velocity maximum [m/s]			Temperature maximum [K]
		bottom of channel loop inner surface	maximum at x=0	in ICF	Channel outlet	Interface of throat and bath	
Original	231.5	1.52	1.69	1.71	1.7	1.5	1805
1	236.6	1.50	1.90	1.69	1.5	1.3	1827
2	227.7	1.60	1.64	1.69	1.7	1.4	1810

Velocity profiles. The steady-state velocity distributions in channel loop are similar (Figures 5a, 5b, 5c) and maximal values of velocity are very close (Table 1) for all three models. It is clear because there are no changes of geometry in considered element of ICF construction.

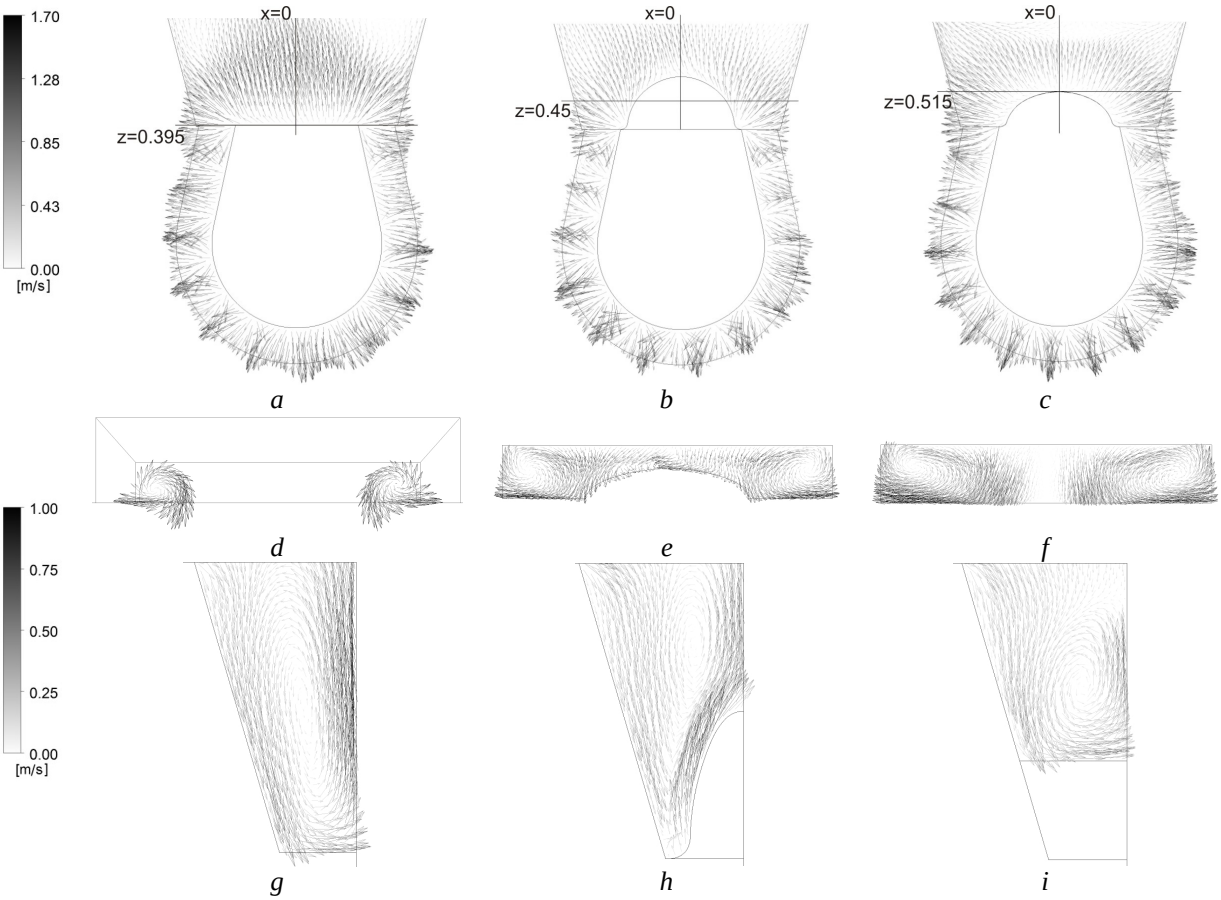

Figure 5. Steady-state velocity vectors distribution for original model (a,d,g), model 1 (b,e,h) and model 2 (c,f,i) for cross-sections y=0 (a,b,c), horizontal cross-sections z=0.395 (d), z=0.45 (e), z=0.515 (f) as well as for cross-section x=0 (g,h,i) in zone of throat with sediments.

Flow patterns in horizontal cross-sections, which intersect "hill" (model 1) and "bank" (model 2) zones (see for example Figure 5e) are similar to zones of channel outlets z=0.395 (Figure 5d). Thus these zones of sediments in the throat bottom may be considered as channel extension.

Flow patterns above clogging zones (Figure 5a) are similar to flow patterns above channel outlets for original model [2] with characteristic four contours of circulation or two contours of circulation if computed model represent only half of ICF symmetrical geometry.

For the "hill" there is roundabout way for stream lines (Figure 5h). For the "bank" the closure of flow patterns is performed in smaller volume (Figure 5i).

For the side cross-sections, which are close to slant surface of the throat, the horizontal component of velocity is increasing in comparison to vertical component. This may be explained by closeness of channel outlet with its characteristic circulation (Figure 5d).

Figures 5a, 5b, 5c show, that HD field, obtained with SST k-ω model of turbulence, has the regular structure of different intensities' flow patterns in cross-sections, which are perpendicular to channel longitudinal axis. The step of flow structures' repetition is approximately $\alpha \sim 20^{o}$–25^{o}. As similar structures are not obtained with experimentally verified LES model (see, for example [2]), it is the illustration, that two parameter model of turbulence cannot represent proper detailed spatial structure of substantially transient turbulent flow.

The comparison of computationally obtained (Figure 5) and experimentally measured [6] (Figure 6) velocity vectors show qualitative similarity of flow patterns:

– the direction of circulation

– number of circulation contours.

Such qualitative comparison is quite acceptable for ICF with single induction unit despite of difference of geometry parameters.

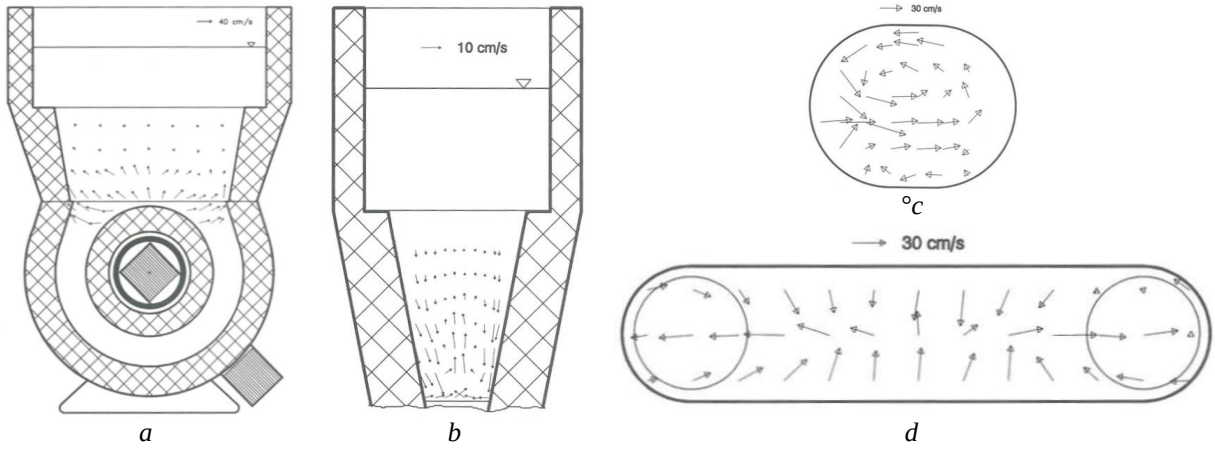

Figure 6. Measured velocity vectors distribution for experimental setup [6]: frontal cross-section of ICF (a), side cross-section of throat and bath (b); cross-section of channel outlet (c), horizontal cross-section of throat (d).

Temperature field. The positions of temperature maximum for original model and model 1 are in the right channel branch – opposite to position of Joule heat maximum in the left channel branch. The temperature maximum for model 1 is for 20K greater in comparison with original model. The cause of local overheating for model 1 is the concentration of Joule heat power in zone of "hill" base (Figure 4e).

As to model 2 the maximum of temperature is shifted to the outlet of the left channel zone (Figure 7), the value of temperature maximum is for 5K greater than in original model despite of the smaller integral Joule heat power (Table 1). This may be explained with the considerably changed thermal exchange in throat with sediments with the form of "bank" because of smaller depth of the throat.

Figure 7. Temperature steady-state distributions for original model (a), model 1 (b) and model 2 (c)

Conclusions:

– The clogging of throat bottom may be cause of noticeable concentration of Joule heat power in zones near sediments and thus may be cause of re-distribution of integral Joule heat power between various ICF zones.

– The non-conductive sediments at the throat bottom may be cause of noticeable local overheating of melt, which may shorten the effective operation period of industrial ICF.

– The computations of ICFs with clogging are to be continued especially for the cases with ICF channel with sediments as the presented results for melt flow and temperature field are only the initial trials of computational models for ICF with clogging.

– For melt flow and thermal field modelling LES approach is to be applied as two-dimensional model make possible only qualitative estimations of integral HD and thermal parameters of industrial ICF.

Acknowledgements

The current research was performed with the financial support of the ESF project of the University of Latvia, contract No. 2009/0223/1DP/1.1.1.2.0/09/APIA/VIAA/008.

REFERENCES

1. Baake E., Jakovics A., Pavlovs S., Kirpo M. Numerical Analysis of Turbulent Flow and Temperature Field in Induction Channel Furnace with Various Channel Design // International Scientific Colloquium “Modelling for Material Processing”, Riga, September 16-17, 2010, pp. 253–258.
2. Baake E., Jakovics A., Pavlovs S., Kirpo M. Long-term computations of turbulent flow and temperature field in the induction channel furnace with various channel design // Magnetohydrodynamics – 2010, Vol. 46, Nr. 4, pp. 317–330.
3. Jakovics A., Pavlovs S., Kirpo M., Baake E. Long-term LES Study of Turbulent Heat and Mass Exchange in Induction Channel Furnaces with Various Channel Design // Fundamental and Applied MHD, Borgo, Corsica, France, 2011, vol. 1, pp. 283–288.
4. Baake E., Jakovics A., Pavlovs S., Kirpo M. Influence of channel design on heat and mass exchange of induction channel furnace // COMPEL (The International Journal for Computation and Mathematics in Electrical and Electronic Engineering), 2011, Vol. 30, No. 5, pp. 1637–1650.
5. Pavlovs S., Jakovics A., Baake E., Nacke B., Kirpo M. LES modelling of turbulent flow, heat exchange and particles transport in industrial induction channel furnaces // Magnetohydrodynamics – 2011, Vol. 47, Nr. 4, pp. 399–412.
6. Eggers, A. Untersuchungen der Schmelzenströmung und des Wärmetransports im Induktions-Rinnenofen, Fortschritt-Berichte VDI, Düsseldorf, 1993, 152 S.